# Modelling Of Characteristic Parameters for Asymmetric DHDMG Mosfet

SWAPNADIP DE
Department of ECE,
Meghnad Saha Institute of Technology,
Nazirabad, Kolkata-700107, INDIA

and

ANGSUMAN SARKAR
ECE Department
Kalyani Government Engineering College, Kalyani-741235, INDIA

and

CHANDAN KUMAR SARKAR
ETCE Department
Jadavpur University, Kolkata-700032, INDIA
swapnadipde26@yahoo.co.in

*Abstract:* A quasi-Fermi potential based analytical subthreshold drain current model for linear profile based DHDMG MOS transistor, incorporating the fringing fields at the two ends of the device, without the use of any fitting parameter as is the case with drift-diffusion approach is proposed. The model uses an average doping concentration expression. A pseudo-2D analysis applying Gauss' law along the surface is used to model the subthreshold surface potential. The same model is used to find the threshold voltage and drain current for Gaussian profile based DHDMG. A detailed comparison of the proposed Gaussian model with the previously proposed linear model is also presented. The proposed model is also compared with Double gate MOSFET and better performance in terms of DIBL effect reduction is observed. The results obtained are compared with a 2D device simulator DESSIS. Very good agreement of the results from DESSIS with those from the proposed model validates the model for suppressing the short channel effects.

*Key-Words*: Drain Current; Threshold Voltage; Surface Potential; Pseudo Analysis; Halo; Dhdmg.

## 1 Introduction

Bulk MOSFETs show the severe short channel effects like drain induced barrier lowering (DIBL) and threshold voltage roll-off as the channel length of device goes down in sub-50 nm regime. The controllability of the gate voltage on the channel charge degrades severely as a result. DHDMG MOSFETs are the good candidate to replace the conventional MOSFETs in this particular region because of their excellent immunity to the short channel effects.

When the gate electrode is biased below the threshold voltage, and also the conducting channel is weakly inverted we say that a MOSFET structure is in subthreshold region. Here the off state leakage current increases due to source and the barrier of the channel to the drain voltage i.e., drain induced barrier lowering takes place. This effect is known as short channel effect which arises due to high electric field in the channel region. In analog applications, the devices have higher gain because of the higher transconductance-to-current ratio in the subthreshold region. The subthreshold regime is also very important in digital applications. When the gate bias is above threshold, a significant drain current pass through the MOSFET device and it is called on-state. The off-state, which corresponds to a subthreshold gate bias, should ideally block all drain current. But there will always be some leakage current in the off-state or in subthreshold regime. So we need an accurate model in this region to characterize the circuit behavior based on subthreshold operation of the devices.

In this paper a quasi-Fermi potential based analytical subthreshold current model for sub 50 nm DHDMG MOSFET has been derived taking into consideration linear and Gaussian variation of the doping profile of the two pockets. Here an average

doping profile concentration expression is considered for deriving the drain current and threshold voltage expression. Simulation results show that the model predicts the value of the drain current fairly accurately for different device and halo profile parameters along with various bias voltages. It proves the validity and usefulness of the proposed model for circuit simulation of ULSI devices. The model is also compared with conventional multigate devices like Double gate. Better performance of the proposed model in terms of short channel effect reduction is observed. The results prove the validity of our model for analog circuits in 40 nm subthreshold regime.
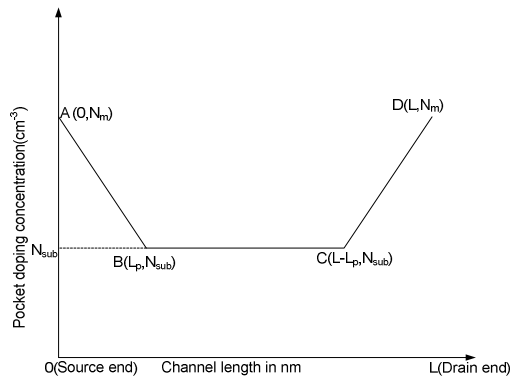
## 2 Model descriptions



Figure1: Plot of pocket doping concentration v/s channel length for DHDMG MOSFET structure

The maximum doping concentration for the halos at the two ends is $N_m$, as is evident from the points A and D in Figure 1.The doping concentration decreases from the maximum value at the source and the drain ends to the substrate doping concentration $N_{sub}$ , linearly along the channel. The linear equation in the source side can be found from the equation of straight line AB, the end co-ordinates for which are given by $(0, N_m)$ and $(L_p, N_{sub})$.Let $(x,y)$be the x-coordinate and y-coordinate respectively.So

$$\frac{y-y_1}{x-x_1}=\frac{y_1-y_2}{x_1-x_2}$$

$$\frac{y-N_m}{x-0}=\frac{N_m-N_{sub}}{0-L_p}$$

$$-L_p y+N_m L_p=N_m x-N_{sub}x$$

$$y=N_{sub}(x/L_p)+N_m(\frac{L_p-x}{L_p})$$

The y-coordinate need to be replaced by the substrate doping concentration at the source end: $N_{sub,S}$ .So we can write

$$N_{sub,S}=N_{sub}(x/L_p)+N_m(\frac{L_p-x}{L_p})$$

For the drain end let the two end point co-ordinates of the straight line CD be $(L, N_m)$ and $(L-L_p, N_{sub})$.So the straight lineequation can be written as

$$\frac{y-N_m}{x-L}=\frac{N_m-N_{sub}}{L-(L-L_p)}$$

$$L_p y-N_m L_p=(N_m-N_{sub})(x-L)$$

$$L_p y=(N_m-N_{sub})x+N_m(L_p-L)+N_{sub}L$$

$$y=N_{sub}(\frac{L-x}{L_p})+N_m(\frac{L_p-L+x}{L_p})$$

For the drain end instead of y we can write $N_{sub,D}$.

$$N_{sub,D}=N_{sub}(\frac{L-x}{L_p})+N_m(\frac{L_p-L+x}{L_p})$$

The doping concentration of region BC is the substrate doping concentration $N_{sub}$.
So the average doping is given by

$$N_{av}=\frac{1}{L}\int_0^L[N_{sub,S}+N_{sub,D}+N_{sub}]dx$$

$$N_{av}=N_{sub}(1+\frac{L}{L_p})+N_m(2-\frac{L}{L_p}) \qquad (1)$$

An n-channel DHDMG structure used to implement the model is shown in Figure 2:
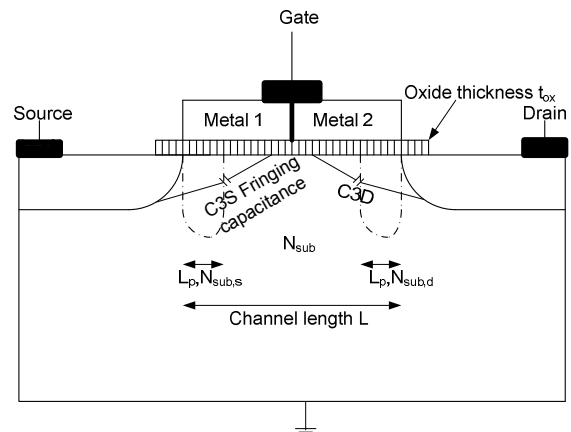


Figure2: An n-channel linear profile based DHDMG MOSFET structure.

An elementary Gaussian box is considered at a position x along the channel of length $\Delta x$ as in [1] and [2].The height of the box is so chosen that it

covers the entire depletion depth. The width of the box is taken equal to the gate width. So if $Y_d$=the depletion depth and $W$=width of the rectangular box then the volume of the elementary box is $\Delta x Y_d W$.

If $\varepsilon$=the permittivity of the dielectric medium trhen applying Gauss law to the box gives

$$\varepsilon \oint \vec{E}.\vec{ds} = -qN_{av}Y_d \Delta x W$$

Where $\vec{E}$ stands for the electric field striking the faces of the box perpendicularly. $\vec{ds}$ stands for the area of the faces of the box. If $\varepsilon_{Si}$ and $\varepsilon_{ox}$ be the permittivity of Silicon and silicon dioxide respectively we get

$$\varepsilon_{si}\frac{d^2\psi_s}{dx^2} - \frac{C_{ox}}{Y_d}\psi_s = qN_{av} - \frac{C_{ox}}{Y_d}V_{GS}' \qquad (2)$$

Where $\frac{\varepsilon_{ox}}{t_{ox}} = C_{ox}$ stands for the oxide capacitance per unit gate area. The typical variation of the depletion layer depth is shown below as in[4]:
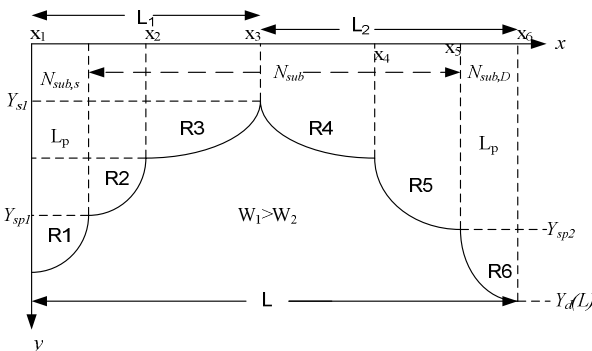


Figure3:Variation of depletion layer depth along the channel.

The above equation needs to be solved for perfect estimation of the surface potential as in [3],[4]. However since $Y_d$ is a function of x so $Y_d(x)$ need to be modelled for obtaining a perfect solution of the surface potential.

A model of $Y_d(x) = (ax+b)^2$ is proposed where the source and the drain end values are given by

$$Y_d(0) = X_j + \sqrt{2\varepsilon_{si}(V_1)/(qN_{av})} = X_j + X_{rs}$$

and

$$Y_d(0) = X_j + \sqrt{2\varepsilon_{si}(V_7)/(qN_{av})} = X_j + X_{rd}$$

respectively where, $V_1 = V_{SB} + V_{bi} + V_{fs}$, $V_7 = V_{DB} + V_{bi} + V_{fd}$,

$V_{bi}$ is the built-in potential of the substrate. $V_{SB}$ and $V_{DB}$ are the source and the drain bias

respectively, $N_{av}$ is the average concentration,

$$X_{rs} = \sqrt{2\varepsilon_{si}(V_1)/(qN_{av})}$$ and

$$X_{rd} = \sqrt{2\varepsilon_{si}(V_7)/(qN_{av})}$$

are the depth of penetrations of the depletion layers into the channel / substrate due to the built-in potential $V_{bi}$ (between the $n^+$ -source/drain and the p-type channel/substrate) and the reverse bias $V_{SB}$ and $V_{DB}$ at the source and the drain ends .

The channel is divided into six regions with known values $V_1$ and $V_7$ at the two ends. The unknown voltages are obtained by applying the continuity of the electric field along the lateral direction $\frac{d\psi_s}{dx}$ at the junction of the different regions. The following simultaneous equations are obtained which are solved for obtaining the unknown voltages.

$$a_{11}V_2 + a_{12}V_3 + a_{13}V_4 + a_{14}V_5 + a_{15}V_6 = A_1$$
$$a_{21}V_2 + a_{22}V_3 + a_{23}V_4 + a_{24}V_5 + a_{25}V_6 = A_2$$
$$a_{31}V_2 + a_{32}V_3 + a_{33}V_4 + a_{34}V_5 + a_{35}V_6 = A_3$$
$$a_{41}V_2 + a_{42}V_3 + a_{43}V_4 + a_{44}V_5 + a_{45}V_6 = A_4$$
$$a_{51}V_2 + a_{52}V_3 + a_{53}V_4 + a_{54}V_5 + a_{55}V_6 = A_5$$

The co-efficients are obtained by solving the above equations.

Two bias depenedent fitting parameters $\zeta_s = V_1 / V_{bi}$ for the source end and $\zeta_d = V_7/V_{bi}$ for the drain end are considered for obtaining a best fit model of surface potentail profile with ISE TCAD. The depth of the six depletion regions are obtained as in [4] replacing $N_p$ and $N_a$ by $N_{av}$. The surface potentials for all the regions can be determined similarly from (2). The same model can be applied for estimation of surface potential for SHDMG device[5].

The five regions in which the channel is divided for SHDMG are as follows:

**Region-I** : $x_1 = 0 < x \leq x_2 = L_p$ The corresponding $y$ values are $y_1 = \left\{ X_j + \sqrt{2\varepsilon_{si}V_1/(qN_{av})} \right\}/\varsigma_s$ and

$y_2 = Y_{sp1} = \sqrt{2\varepsilon_{si}\psi_{sp1}/(qN_{av})}$ with the end potentials $V_1 = V_{bi} + V_{SB} + V_{fs}$ and $V_2$ to be

evaluated $\psi_{sp1} = \left( -\gamma_p/2 + \sqrt{\gamma_p^2/4 + V_{GB} - V_{FBP1}} \right)^2$,

$\gamma_p = \sqrt{2q\varepsilon_{si}N_{av}}/C_{ox}$, $V_{FBP1} = V_{FBP} - V_{FB1}$    and

$V_{FBP} = -0.56 - \varphi_t \ln(N_{av}/n_i)$

**Region-II** : $x_2 < x \leq x_3 = x_{rs}$ : The corresponding $y$ values are $y_2 = Y_{sp1}$ and $y_3 = Y_{sp} = \sqrt{2\varepsilon_{si}\psi_{sp}/(qN_{av})}$

where $\psi_{sp} = \left(-\gamma_p/2 + \sqrt{\gamma_p^2/4 + V_{GB} - V_{FBP}}\right)^2$

**Region-III** : $x_3 < x \le x_4 = L1$ : The corresponding $y$ values are $y_3 = Y_{sp}$ and $y_4 = Y_{s1} = \sqrt{2\varepsilon_{si}\psi_1/(qN_{av})}$ where

$$\psi_1 = \left(-\gamma/2 + \sqrt{\gamma^2/4 + V_{GB} - V_{FB1}}\right)^2$$

$$\gamma = \sqrt{2q\varepsilon_{si}N_{av}}/C_{ox}$$

**Region-IV** : $x_4 < x \le x_5 = (L1+L2)0.75$ : The corresponding $y$ values are $y_4 = Y_{s1}$ and

$$y_5 = Y_{s2} = \sqrt{2\varepsilon_{si}\psi_2/(qN_{av})}$$

where $\psi_2 = \left(-\gamma/2 + \sqrt{\gamma^2/4 + V_{GB} - V_{FB2}}\right)^2$

**Region-V** : $x_5 < x \le x_6 = L$ : The corresponding $y$ values are $y_5 = Y_{s2}$ and

$$y_6 = \left\{X_j + \sqrt{2\varepsilon_{si}V_6/(qN_{av})}\right\}/\varsigma_d$$

The surface potential $\Psi_s(x)$ for all the five regions are determined. Applying the continuity of the Electric Field along the lateral direction ($d\Psi_s/dx$) at the interfaces of the various regions we get :

$a_{11} V_2 + a_{12} V_3 + a_{13} V_4 + a_{14} V_5 = A_1$

$a_{21} V_2 + a_{22} V_3 + a_{23} V_4 + a_{24} V_5 = A_2$

$a_{31} V_2 + a_{32} V_3 + a_{33} V_4 + a_{34} V_5 = A_3$

$a_{41} V_2 + a_{42} V_3 + a_{43} V_4 + a_{44} V_5 = A_4$

## 2.1 Drain current model

The drift-diffusion model for drain current as [4] requires a fitting parameter $\eta'$. The quasi-Fermi potential based model eliminates the need of any such fitting parameter and hence gives a more accurate estimation of the drain current.

The total current density for the current flowing from the drain to the source end is given by

$$J_n = -n\mu_n \frac{dE_{F_n}}{dx}. \tag{3}$$

$E_{F_n}$ stands for the Quasi-Fermi potential for electrons.

If the inversion layer hole density is taken as $p$

$$np = n_i^2 e^{\{(E_{F_n} - E_{F_p})/q\Phi_t\}}$$

Also considering $N_{av}$ as the average channel doping concentration,

$$p = N_{av} e^{-\Psi_s/\Phi_t}$$

$$n = \frac{n_i^2}{N_{av}} \frac{e^{\{(E_{F_n} - E_{F_p})/q\Phi_t\}}}{e^{(-\Psi_s/\Phi_t)}}$$

$$J_n = -\mu_n (\frac{n_i^2}{N_{av}}) \frac{e^{\{(E_{F_n} - E_{F_p})/q\Phi_t\}}}{e^{(-\Psi_s/\Phi_t)}} \frac{dE_{F_n}}{dx} \tag{4}$$

Also from [4],

$$\delta = \frac{\Phi_t}{E_y} = \Phi_t\sqrt{\varepsilon_{Si}/(2qN_{av}\psi_s)}$$ , considering the average concentration.

Also $I_{DS} = J_n W\delta$.

So

$$I_{DS} = -\mu_n W (\frac{n_i^2}{N_{av}}) \frac{e^{\{(E_{F_n} - E_{F_p})/q\Phi_t\}}}{e^{(-\Psi_s/\Phi_t)}} \Phi_t\sqrt{\varepsilon_{Si}/(2qN_{av}\Psi_s)} \frac{dE_{F_n}}{dx}$$

$$I_{DS} = -\mu_n W \eta' \frac{e^{\{(E_{F_n} - E_{F_p})/q\Phi_t\}}}{\sqrt{\Psi_s}e^{(-\Psi_s/\Phi_t)}} \Phi_t\sqrt{\varepsilon_{Si}/(2qN_{av}^3)} \frac{dE_{F_n}}{dx}$$

The splitting of the electron quasi-Fermi levels on the source side by ($V_{SB} + V_{fs}$) gives the applied bias in the source end as

$$E_{F_n} - E_{F_p} = -q(V_{SB} + V_{fs})$$

For the drain end

$$E_{F_n} - E_{F_p} = -q(V_{SB} + V_{DS} + V_{fd}) = -q(V_{DB} + V_{fd})$$

Where $V_{DS}$ is the drain bias. So

$$I_{DS} = -\mu_n W \eta' \frac{e^{[-\{(V_{SB} + V_{fs})/\Phi_t\}/q\Phi_t]}}{\sqrt{\Psi_s}e^{(-\Psi_s/\Phi_t)}} \Phi_t\sqrt{\varepsilon_{Si}/(2qN_{av}^3)} \frac{dE_{F_n}}{dx}$$

The total subthreshold drain current is obtained by integrating x from 0 to L, the channel length.

$$I_{DS} = -\mu_n W \eta' \frac{e^{-\{(V_{SB} + V_{fs})/\Phi_t\}}}{\int\sqrt{\Psi_s}e^{(-\Psi_s/\Phi_t)}dx} \Phi_t^2\sqrt{q\varepsilon_{Si}/(2N_{av}^3)}\{1 - e^{-(V_{DS} + V_{fd})/\Phi_t}\} \tag{5}$$

Numerical techniques can compute the denominator.

From [3], the transconductance $g_m$ and $I_{DS}$ are related by

$$\frac{g_m}{I_{DS}} = \frac{\Phi_t}{m}$$ where m>1.

Since $I_{DS}$ is more for DHDMG and SHDMG compared to DMG, so the value of $g_m$ is more in DHDMG than DMG. The increase in the drain current for DHDMG is attributed to the fact that the velocity of electrons increases in the source and the drain ends and hence the carrier transport efficiency is improved. $\frac{g_m}{I_{DS}}$ is more in subthreshold regime than superthreshold. So the gain of a circuit in the subthreshold regime is more.

## 2.2 Model of DHDMG based on Gaussian pocket doping profile

For practical MOSFETs the linear and constant doping profile are replaced by Gaussian distributed doping profile in the channel due to the requirement of many implantation and diffusion steps during fabrication process, such as threshold adjust implantation. So modeling of surface potential, threshold voltage and drain current with a Gaussian doping profile may provide some better physical characteristics of real DHDMG MOSFETs.
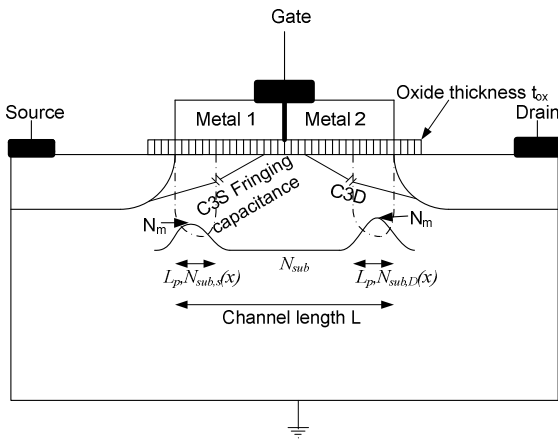


Figure 4: An n-channel Gaussian profile based DHDMG MOSFET structure

The basis of the model is to assume two Gaussian profiles as in [7] at the source and drain edges given in Figure4. The Gaussian profile at the source side is given by:

$$N_{sub,S}(x) = N_m e^{-\{(x/L_p)\}^2}$$

x represents the distance across the channel.

$N_m$ and $L_p$ stands for the maximum doping concentration of the Gaussian profile and the horizontal length of the Gaussian halo doped regions.The Gaussian profile is assumed symmetrical for the source and the drain edges for the DHDMG device.

The drain end profile is given by

$$N_{sub,D}(x) = N_m e^{-\{(L-x)/L_p\}^2}$$

Considering $N_{sub}$ as the uniform substrate doping the average concentration is given by

$$N_{av,Gauss} = \frac{1}{L} \int_0^L [N_{sub,S}(x) + N_{sub,D}(x) + N_{sub}]dx$$

$$N_{av,Gauss} = \frac{\int_0^L [N_m e^{-\{(x/L_p)\}^2} + N_m e^{-\{(L-x)/L_p\}^2} + N_{sub}]dx}{L}$$

$$N_{av,Gauss} = N_{sub} + \frac{L_p}{L} N_m [\int_0^{\frac{L}{L_p}} e^{-p^2} dp - \int_{\frac{L}{L_p}}^0 e^{-p^2} dp]$$

$$N_{av,Gauss} = N_{sub} + N_m \{\frac{sqr(\pi) erf(\frac{L}{L_p})}{\frac{L}{L_p}}\} \qquad (6)$$

From (6) the final average concentration term is an error function of its effective channel length as well as the maximum doping concentration of the sour and drain end Gaussian profiles and the pocket length at the two ends.

The surface potential for this Gaussian doping distribution profile can be computed from the following equation:

$$\varepsilon_{si} \frac{d^2\psi_s}{dx^2} - \frac{C_{ox}}{Y_d}\psi_s = qN_{av,Gauss} - \frac{C_{ox}}{y_d}V_{GS}'$$

Where the symbols have their usual significances.
Since( $L/L_p$) is positive and greater than 1 so for any value of $N_m$ and $N_{sub}$ we get a definite value of $N_{av,Gauss}$.

So the above equation can be solved as in [4] to get a definite value of the surface potential for DHDMG devices.

Using the above surface potential model,the threshold voltage $V_T$ which is the gate voltage $V_{GS}$ at which the minimum value of the subthreshold surface potential

$$\psi_{S,min} = 2*\phi_F + V_{SB} + V_{fs}$$ is found out.

Now $x_{min}$ corresponding to $\psi_{S,min}$ is approximated at the junction of regions 2 and 3 or regions 3 and 4. Hence, an iterative numerical method is applied to find the value of threshold voltage.

The subthreshold drain current for this Gaussian doping profile DHDMG can be estimated from

$$I_{DS} = -\mu_n W \hbar_t^2 \frac{e^{-\{(V_{SB}+V_{fs})/\Phi_t\}}}{\int \sqrt{\Psi_s} e^{(-\Psi_s/\Phi_t)} dx} \Phi_t \sqrt{q\varepsilon_{Si}/(2N_{av,Gauss}^\beta)}\{1 - e^{-(V_{DS}+V_{fd})/\Phi_t}\}$$

## 3 Results

Numerical simulations of the DHDMG structure are carried out using a numerical device simulator DESSIS of Synopsys TCAD. This 2-D numerical device simulator can provide most accurate solutions of the 2-D Poisson's equation. Metallic

gates are used for the DHDMG structure shown in Figure2 and Figure4. The n-type poly-silicon is used for the source and drain contacts and the body contact is made of p-type poly-silicon. A wide variation of the device dimensions, with different technology parameters and biasing conditions are used to verify the drain current model against the 2-D numerical device simulator, DESSIS. Unless otherwise mentioned equal values of length of gate metal $M_1(L_1)$ and $M_2(L_2)$ are taken. Similarly unless mentioned otherwise default values of work functions for the two metals taken are $W_1$=4.2 eV and $W_2$=4.1 eV respectively.
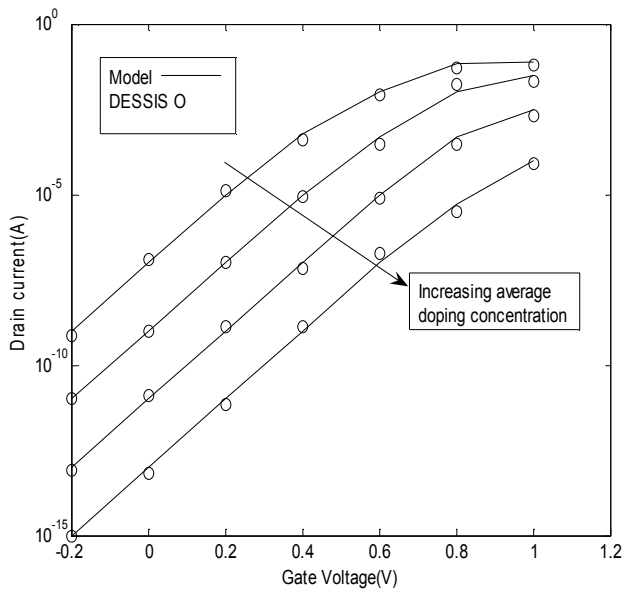


Figure5: Drain current v/s gate voltage plots for linear profile based DHDMG taking L=40 nm, $L_p$=10 nm, $V_{SB}$=0.1V, $V_{DS}$=0.5V with $N_{av}$ =9*10$^{17}$ ,1.2*10$^{18}$ , 1.8*10$^{18}$ and 9*10$^{18}$cm$^{-3}$ and $N_{sub}$ =1*10$^{17}$ cm$^{-3}$

It is seen from Figure5 that increase in the average doping concentration means increase in the source and drain pocket doping if the substrate is assumed at a fixed doping value. The heavy doping in the drain side limits the drain field from penetrating into the source region. So the source and drain coupling, which is the main cause of DIBL effect is reduced greatly. Also the gate control of the channel is substantially improved with increase in doping, that is, the short channel effects are reduced. Hence the drain current reduces with increase in the doping concentration.
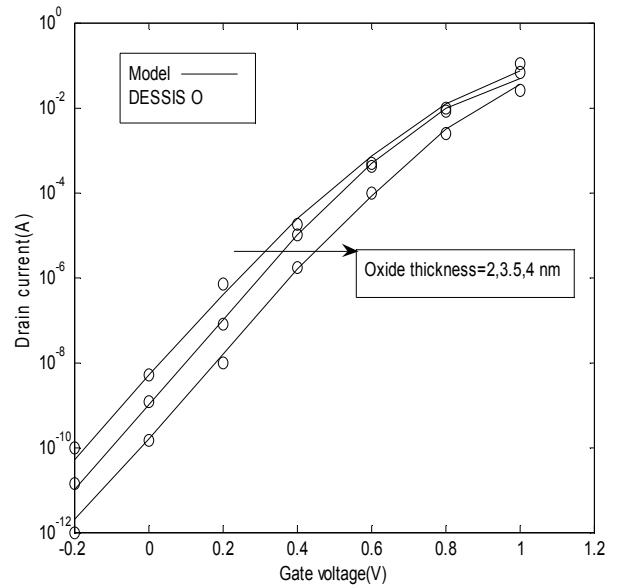


Figure6: Drain current v/s gate voltage for linearly doped DHDMG for L=80 nm, $V_{SB}$=0V,and drain voltage $V_{DS}$ =01V with $N_{av}$ =2*10$^{18}$ cm$^{-3}$, $N_{sub}$ =4*10$^{17}$ cm$^{-3}$, $W_1$=4.25 eV and $W_2$=4.1 eV for three different oxide thicknesses 2,3.5 and 4 nm. It is seen from Figure 6 that as the oxide thickness decreases the electric field from the gate increases. The drain current as a result increases.
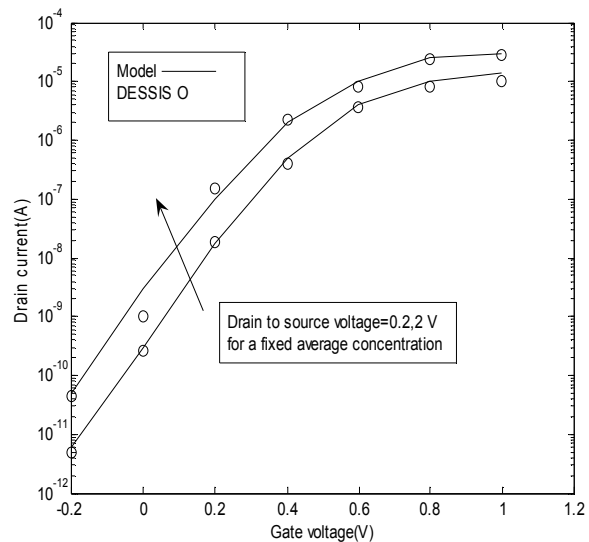


Figure7: Drain current v/s gate voltage plot for linearly doped DHDMG for L=50 nm, $V_{SB}$=0V,and two drain voltages $V_{DS}$ =0.2,2V with $N_{av}$ =1.7*10$^{18}$ cm$^{-3}$ $N_{sub}$ =4*10$^{17}$ cm$^{-3}$.

It is found from Figure 7 that as the drain to source voltage is increased for a fixed value of the gate voltage, the minimum surface potential is elevated, resulting in the significant decrease in the channel

barrier. The electric field from the drain to the source increases. The minimum surface potential shifts towards the source with the increase in the drain-source voltage. The magnitude of surface potential can also be elevated by applying higher gate-source voltage. The results show that the reduction in source-channel barrier, commonly known as drain induced barrier lowering (DIBL) in DHDMG can occur due to the increase in the drain-source voltage. As a result the drain current is increased.
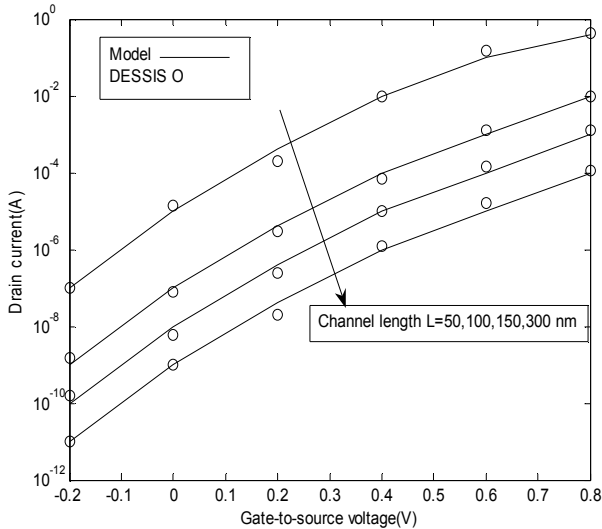
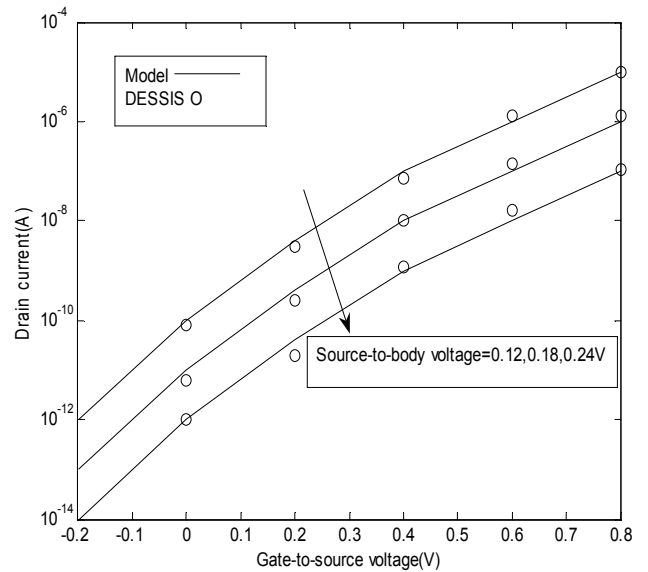voltage $V_{DS}$ =0.2V with $N_{av}$ =1.7*10^{18} cm^{-3} $N_{sub}$ =4*10^{17} cm^{-3} from DESSIS.



Figure10: Drain current v/s gate voltage for linear profile based DHDMG taking L=40 nm, $V_{SB}$ =0V,and drain voltage $V_{DS}$ =1V with $N_{av}$ =4*10^{18} cm^{-3} , $N_{sub}$ =1*10^{17} cm^{-3},for three different source biases 0.12,0.18 and 0.24 V.



Figure8: Drain current versus $V_{GS}$ for linear DHDMG with $L_p$ = 16mm, $N_{av}$ = 1.2 x 10^{18} cm^{-3}, $N_{sub}$ = 6 x 10^{17} cm^{-3}, W1=4.6 eV and W_2=4.25 eV, under the applied bias $V_{SB}$ =0 V, $V_{DS}$ = 1 V for four different effective channel length $L$ = 50,100,150 and 300 nm.
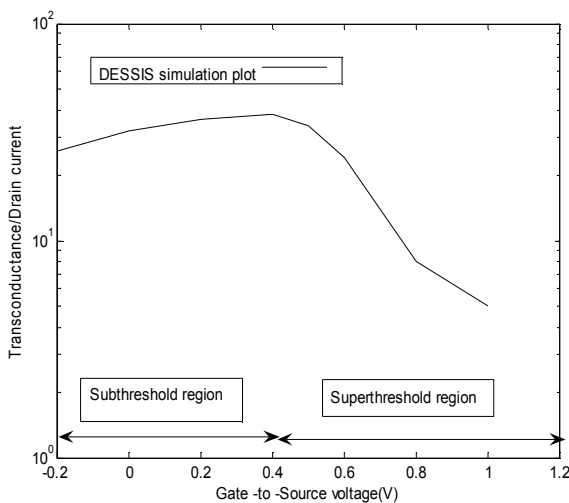


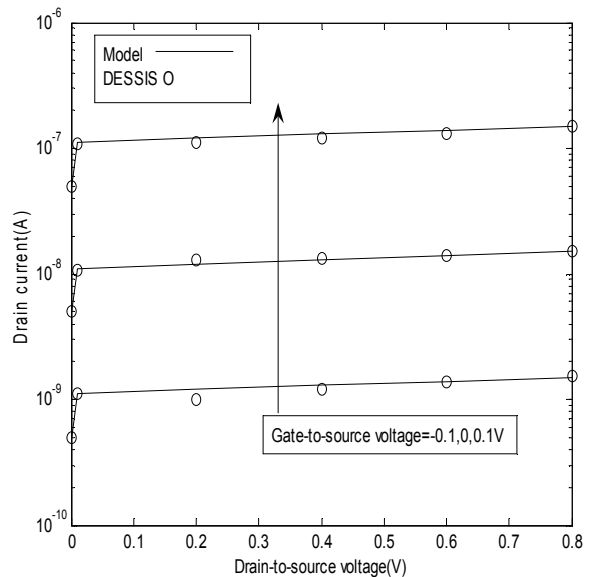Figure9: Plot of $\frac{g_m}{I_{DS}}$ versus gate-to-source voltage for L=50 nm with $V_{SB}$ =0V,and drain



Figure11: Drain current v/s drain-to-source voltage plot for Gaussian profile based DHDMG for L=50 nm, L_p=12nm, $V_{SB}$ =0V,and three gate voltages $V_{GS}$ =-0.1,0,0.1V with $N_{av,Gauss}$ =1.2*10^{18} cm^{-3} and $N_{sub}$ =4*10^{17} cm^{-3}.
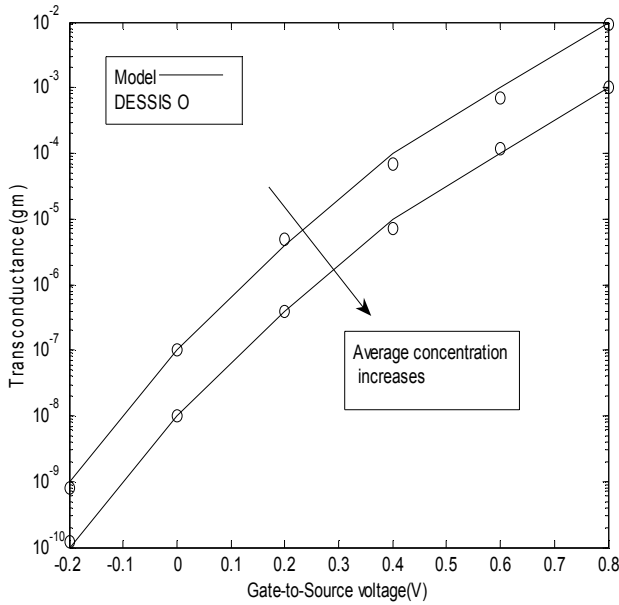
Figure12: Transconductance v/s gate voltage plot for linearly doped DHDMG for L=40 nm, $L_p$=10nm, $V_{SB}$=0V, $V_{DS}$=1V with i) $N_{av}$ =1.2*10^{18} cm^{-3} $N_{sub}$ =1*10^{17} cm^{-3} ii) $N_{av}$ =1.8*10^{18} cm^{-3} $N_{sub}$ =1*10^{17} cm^{-3}

It is seen from Figure 8 that as the channel length decreases the DIBL effect increases. The gate control of the channel is decreased and the drain current increases. Figure 9 shows that $\frac{g_m}{I_{DS}}$ is more in subthreshold regime than superthreshold.So the gain of a circuit in the subthreshold regime is more.

It is seen from Figure 10 that as the source voltage is increased the inversion layer at the channel surface is reduced, and hence for a fixed drain voltage a reduced current level is found as shown in the plots. Since in the subthreshold regime the transconductance is proportional to the drain current so as the drain current decreases with increase in the doping concentration, the transconductance also reduces, as in Figure 11 and Figure 12. So the gain of a circuit in subthreshold region increases as average doping increases.
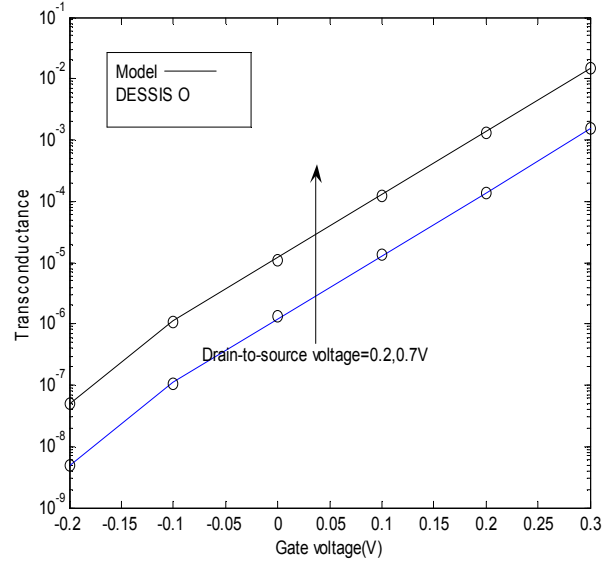


Figure 13: Transconductance v/s gate voltage plot for Gaussian profile based DHDMG for L=40 nm, $L_p$=10nm, $V_{SB}$=0V, $V_{DS}$=1V with $N_{av,Gauss}$ =1.2*10^{18} cm^{-3} $N_{sub}$ =1*10^{17} cm^{-3} for two sets of drain bias.
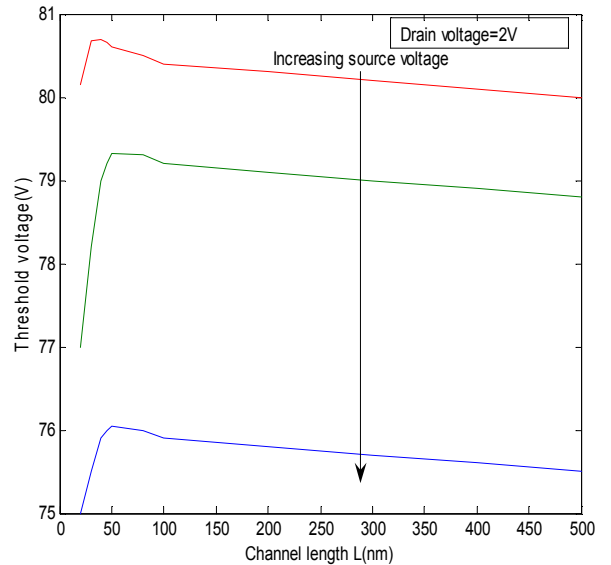


Figure14: Plot of threshold voltage v/s channel length for Gaussian profile based DHDMG for $V_{SB}$ =0.2,0.5 and 1.2 V, $V_{DS}$ = 2 V taking $N_{sub}$ =4*10^{17} cm^{-3}, $N_{av,Gauss}$ =4*10^{18} cm^{-3},$L_p$=14 nm , $W_1$=4.6 eV and $W_2$=4.1 eV.

It is seen from Figure 13 that as the drain bias is increased the drain current increases. The gate control of the channel decreases and the DIBL effect is increased. Since the transconductance is proportional to the drain current so it increases. All the plots in Figure 14 show that the roll-off starts

around 40 nm and so the DHDMG device can be effectively used up to 40 nm. Below 40 nm the Quantum effects are predominant and so the circuit performance will degrade.
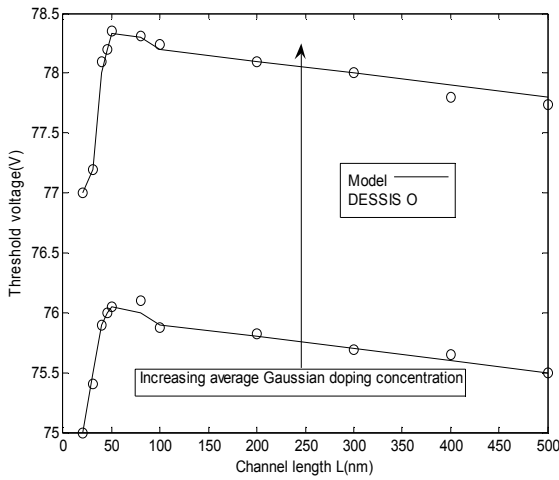


Figure15: Plot showing threshold voltage roll-off v/s channel length for $N_{av,Gauss}$ =1.2*10^{18} cm^{-3} and 9*10^{18} cm^{-3} taking all other parameters same as in Figure 14.

Comparison of the results obtained from DESSIS using the subthreshold current criterion with the Gaussian profile based DHDMG model as in Figure 15 and Figure 16 show that the proposed model is useful to compute the threshold voltage for DHDMG device.
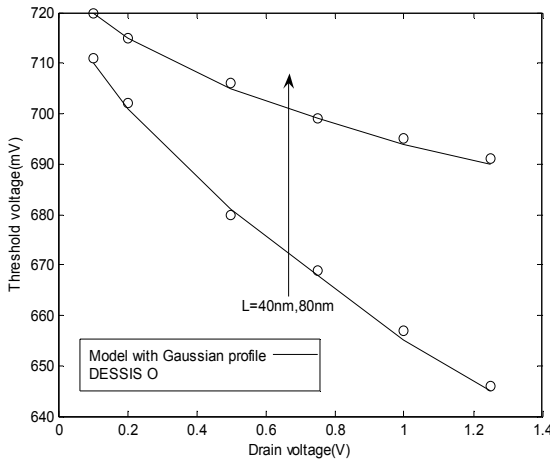


Figure16: Plot of threshold voltage v/s drain bias for a Gaussian profile based DHDMG n-mosfet for $V_{SB}$=0V, $V_{DS}$=1V for two different channel lengths,L=40 and 80 nm,taking $N_{sub}$ =4*10^{17} cm^{-3} , $N_{av,Gauss}$ =4*10^{18} cm^{-3} ,Lp=12 nm.
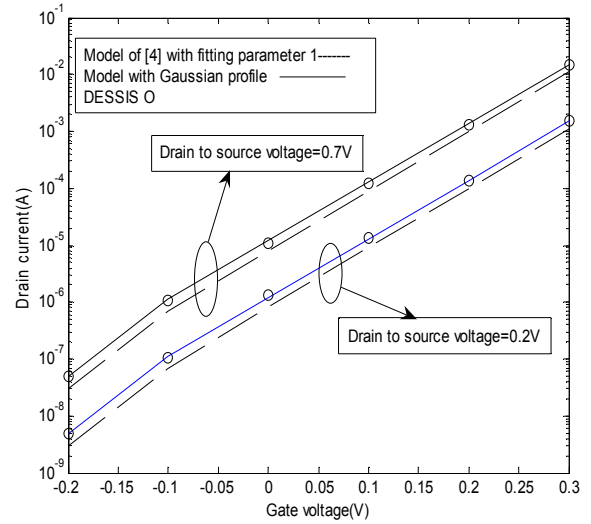


Figure17: Plot of drain current v/s gate voltage for Gaussian profile based DHDMG and model in [4] with fitting parameter taken 1 instead of 1.5 for two different drain biases=0.2 and 0.7V,L=40 nm, Lp=12 nm, keeping the other parameters same as in Figure 16 .

The plots in Figure 17 show that if the fitting parameter in drift-diffusion based model is not considered the drain current results do not tally with the 2D device simulator DESSIS. However the results from the quasi-Fermi based approach is in good agreement with DESSIS.
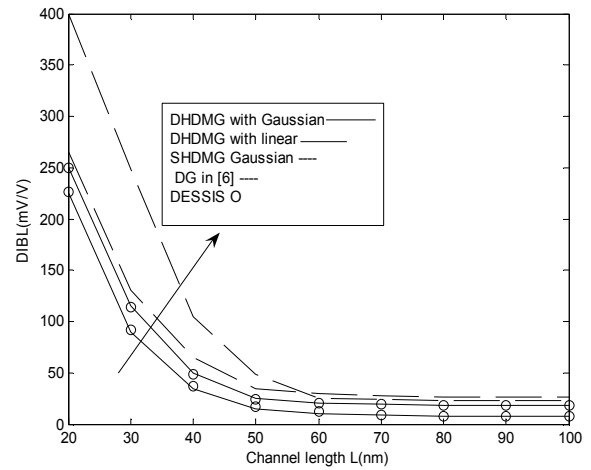


Figure18: Plot of DIBL coefficient v/s channel length for Gaussian profile based DHDMG, linear profile based DHDMG, Gaussian profile based SHDMG and Double gate in [6] taking oxide thickness=2 nm, silicon thickness=20 nm, $N_{av}$ =1.2*10^{18} cm^{-3} and $N_{sub}$ =4*10^{17} cm^{-3} , $N_{av,Gauss}$ =9*10^{18} cm^{-3} , for $V_{SB}$=0V, $V_{DS}$=1V and other parameters same as [6].

It is seen from Figure 18 that the DIBL effect is reduced considerably in DHDMG device for the two doping profiles because of the presence of the two halos at the two ends.

# 4 Conclusion

An analytical quasi-Fermi potential based drain current model for pocket implanted DMG MOSFET is proposed taking into consideration linearly varying pocket doping profiles at the two ends. The model eliminates the need of any fitting parameter as was the case in drift-diffusion theory based drain current models. Further a two dimensional analytical model for the surface potential , threshold voltage and drain current of asymmetric DHDMG MOSFETs with vertical Gaussian doping profile in the channel is also proposed. The model is developed based on two gradual Gaussian doping profiles at the source and the drain ends and further reduced to a useful compact expression. The effects of doping profile parameters and device parameters on the threshold voltage and drain current of the DHDMG devices are discussed. The model results are found to be well matched with the device simulator DESSIS for channel lengths above 40nm. The present model could be useful for determining the subthreshold characteristics of a practical DHDMG n-MOSFET where a Gaussian like doping profile is expected to occur due to many implantation techniques being used during fabrication process.

*References*

[1] Swapnadip De, Angsuman Sarkar, C.K.Sarkar, 'Effect of Fringing Field in Modeling of Subthreshold Surface Potential in Dual Material Gate (DMG) MOSFETS', in ICECE 2008 (Vol. 1), 20–22 December, pp. 148–151, available in IEEE Xplore.

[2] Angsuman Sarkar, Swapnadip De, Nagarajan, M., C.K.Sarkar and S.Baishya, 'Effect of Fringing Fields on Subthreshold Surface Potential of Channel Engineered Short Channel MOSFETs', in Tencon 2008, IEEE Region 10 Conference, 19–21 November, pp. 1–6, available in IEEE Xplore.

[3] Angsuman Sarkar., Swapnadip De and C.K.Sarkar, VLSI Design and EDA Tools (1st ed.), SciTech Publications. (ISBN 978 81 8371 452 5).

[4] Swapnadip De, Angsuman Sarkar, C.K.Sarkar, 'Modelling of parameters for asymmetric halo and symmetric DHDMG n-MOSFETs ', International Journal of Electronics, Taylor and Francis, volume 98, no.10, pp.1365-1381.

[5] Kumar, M.J., and Chaudhry, A. (2004), 'Two-Dimensional Analytical Modeling of Fully Depleted SHDMG SOI MOSFET and Evidence for Diminished SCEs', IEEE Transactions on Electron Devices, 51, 569–674.

[6] Tsormpatzoglou, A., Dimitriadis, C.A., Clerc, R., Pananakakis, G., and Ghibaudo, G. (2008), 'Threshold Voltage Model for Short-Channel Undoped Symmetrical Double-Gate MOSFETs', IEEE Transactions on Electron Devices, 55, 2512–2516.

[7] Pramod Kumar Tiwari, S.Jit (2008), 'Threshold Voltage Model for Symmetric Double-Gate(DG) MOSFETs with non-uniform doping profile', Journal of Electron Devices , 7, 241-249.